



**HAL**  
open science

## Modeling and simulation of sparking in fastening assemblies.

L. Chemartin, P. Lalande, F. Tristant

► **To cite this version:**

L. Chemartin, P. Lalande, F. Tristant. Modeling and simulation of sparking in fastening assemblies..  
ICOLSE 2013, Sep 2013, SEATTLE, United States. hal-01058554

**HAL Id: hal-01058554**

**<https://onera.hal.science/hal-01058554>**

Submitted on 27 Aug 2014

**HAL** is a multi-disciplinary open access archive for the deposit and dissemination of scientific research documents, whether they are published or not. The documents may come from teaching and research institutions in France or abroad, or from public or private research centers.

L'archive ouverte pluridisciplinaire **HAL**, est destinée au dépôt et à la diffusion de documents scientifiques de niveau recherche, publiés ou non, émanant des établissements d'enseignement et de recherche français ou étrangers, des laboratoires publics ou privés.

## Modeling and simulation of sparking in fastening assemblies

L. Chemartin<sup>1</sup>, P. Lalande<sup>1</sup>, and F. Tristant<sup>2</sup>

<sup>1</sup> ONERA, Chatillon, France,

<sup>2</sup> Dassault Aviation, St Cloud, France

[Laurent.chemartin@onera.fr](mailto:Laurent.chemartin@onera.fr)

### ABSTRACT

This paper deals with modeling and simulation of sparking occurrence in fastening assemblies. The principle consists to calculate in three dimensions the distributions of current density and temperature in the structure over time, and to derive some physical criteria to estimate the possibility of sparking occurrence.

Simulations are performed with a Finite Volume Method in time domain and an unstructured mesh. Low frequency assumption is considered for the calculations of electromagnetic quantities (quasi static assumption). The contact resistances between each elements of the structure are also considered, assuming a uniform distribution of the resistance on the interfaces. The two main mechanisms involved in the not-linear behavior of the fastener during high current components are also modeled. First, dielectric breakdowns of sealant layers are simulated with their dielectric strength. Two different situations are simulated. In the case of a direct attachment of the lightning arc on the fastener, the current enters the assembly through the bolt. In the case of conduction, the current (fraction of D component) passes from the skin to the rib through the bolt. The results of simulations bring to light the role of the contact resistances between the bolt and other elements (rib, skin, nut...) on the occurrence of sparking. In some case, computations indicate some important reinforcements of the current density of more than 10kA/mm<sup>2</sup>, resulting to a strong local heating of the bolt and a possible sparking occurrence.

### INTRODUCTION

The massive use of composite materials in modern aircraft requires careful consideration regarding how the lightning strike attaches, how the current flows through the structure, and how the current interacts with the structure. The great difference between the electric conductivity of metallic fasteners and the conductivity of composite materials increases the probability of lightning attachments to fasteners. Moreover, the large number of fasteners used in aircraft construction creates conditions for the current to

flow through fasteners by conduction in distant zones of attachment.

Sparking or arcing phenomena are generally observed on fasteners in which a high intensity current flows, with likely hazardous effects in the fuel tank area (1). The direct effects of lightning on fasteners and rivets are generally the source of several physical mechanisms. The occurrence of these mechanisms depends on the material used for the assembly (for example, metal rib with carbon composite), the type of electrical threat (attachment or conduction) and the value of the current.

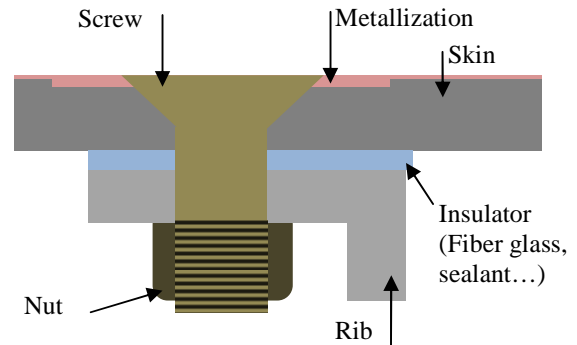


Fig. 1. Schematic drawing of an assembly.

There are three main types of spark that may occur within an assembly. The first one is due to the intense energy spent in internal contacts or small internal voids, which creates high pressure plasma that blows out in the form of sparks. This mechanism, called “outgassing”, is considered to be the most important constraint on fasteners. Moreover, in some cases, the electric field may be reinforced between different pieces (typically the nut and the rib), and a discharge, called “Thermal spark” or “voltage spark” may be created. Finally, some discharges may also occur on the edge of composite ribs. This phenomenon, called “edge glow” is generally associated with the electric field reinforcement between plies oriented differently.

These phenomenons have been widely studied experimentally. However, there is a lack of understanding on the conditions and the

thresholds that create them (2). Experimental study is indeed not easy because of the size, the duration and the intensity of the phenomena. But the large number of kind of fasteners and their associated inherent defaults (manufacturing escape, ageing, in service incident) is the most important issue. It considerably increases the test matrix to be performed for aircraft certification.

The development of a numerical model to simulate sparking conditions may be useful for several reasons:

- It provides data (current density, electric field, temperature) and qualitative features to help the understanding
- It could be used to reduce the test matrix with parametric and relative analyses
- It may be used for the development of instrumentations dedicated for the studies of sparking in fastening assemblies.
- It may help the design of future generations or new concept of assemblies
- It may be derived as macro model for global electromagnetic model

In the first section of this paper, we introduce the numerical model, with all of its assumptions and input data necessary for calculations. The second and third sections present some results in the case of an example of assembly. The second section is focused on the case of arc attachment, and the third in the case of conduction.

## MODEL DESCRIPTION

### Governing Equations

Finite Volume Method is used to solve a set of partial differential equations that model the direct effects of lightning on the assembly. One of the main advantages of the finite volume method is the ability to perform conservative calculations in discontinuous media, as encountered in high intensity arcs (3) and assemblies

Thermal transfers are calculated with the usual heat equation which describes the diffusion of temperature  $T$  (K) in the domain over time. This equation writes:

$$\rho C_p \partial_t T + \vec{\nabla} \cdot \lambda \vec{\nabla} T = S$$

Where  $\rho$  is the density (kg/m<sup>3</sup>),  $C_p$  is the specific heat capacity (J/kg/K),  $\lambda$  is the thermal conductivity (W/m/K) and  $S$  is the source term of Joule heating (W/m<sup>3</sup>). Note that the physical properties of the matter ( $\rho$ ,  $C_p$ , and  $\lambda$ ) are defined

as function of the temperature from a range going from 300K to the boiling point. Thus the energies required for the phase transitions are taken into account through variations of specific heat.

The electrical current distribution over time is calculated with a set of equations derived from the Maxwell equations. The current conservation equation in low frequency approximation writes:

$$\vec{\nabla} \cdot \vec{J} = 0$$

With  $J = \sigma E$  (Ohm's law).  $J$  is the current density (A/m<sup>2</sup>) and  $E$  is the electric field (V/m). In the same way (low frequency), Maxwell Ampere equation writes:

$$\vec{\nabla} \times \vec{B} = \mu_0 \vec{J}$$

where  $B$  (T) is the magnetic field. Those equations are formulated in potentials in order to facilitate the determination of the boundary conditions. The equations on vector potential  $A$  (T/m) are solved with a Crank-Nicholson scheme (2<sup>nd</sup> order).

### Evaporation, ionization and pressure built-up

The physical processes involved in formations of internal sparks are not well understood. Some authors have proposed some models for the calculation of the internal pressure build-up due to sparking (4). This pressure may reach hundreds of bars. Simplest calculations of internal pressure rise over time show that it quickly reaches extremely important values that cannot be held by the assembly. Thus, it is assumed that internal vaporization causes external sparking.

The present model is based on a simple description of the vaporization and ionization process. This approach doesn't pretend to give accurate results, but it gives qualitative information. When the local temperature into a material (or at an interface between two materials) reaches the boiling point, it is assumed that it instantaneously transforms into ionized and conductive gas. It is also assumed that the local electric conductivity became constant, and this process is not reversible. Metallic plasmas, such as aluminum, copper, iron or carbon, reaches indeed electric conductivities of hundreds of S/m just after the vaporization. The conductivity of thermal plasmas never exceeds 10<sup>4</sup>S/m. Thus, the conductivity of vaporized regions is set to 10<sup>3</sup>S/m. In the case of carbon composite, observations of laminates after lighting tests show pyrolyzed fibers and vaporized matrix into the material (5). It is assumed that the ionization

process of the vapor coming from these matters is similar than for metallic material.

### Electric breakdown

A similar approach is used for dielectric breakdown. When the local electric field reaches the dielectric strength into an insulating material (sealant, glass fiber or paint), the material instantaneously transforms into ionized and conductive gas. Experimental observation shows that breakdown occurs very quickly, in few nanoseconds. This process is not reversible. The effect of capacitive current is not taken into account in the breakdown process. Evaluation of the order of magnitude of this component of current indicates it is not sufficient to cause breakdown (low  $dE/dt$ ).

According to the material, the dielectric strength varies from 10kV/mm for alumina to more than 100kV/mm for polyurethane. The following tab shows the typical values used for the calculations.

	Material	Tv (K)	$\sigma$ 300K (S/m)	Ec (kV/mm)
Bolt	Ti6Al4V	3500	6.E+06	-
Rib and Nut	Al2024	2700	3.E+07	-
Metallization	CuSn6	2800	9.E+06	-
Skin	Carbon Fiber	800	1.6E+04	-
Insulator	Polyurethane	730	1.E-12	20
Air	N2O2	-	1.E-14	3

Fig. 2. Materials and basic values used for calculations

Note that electric conductivities of metals decreases when temperature increases, which worsens the effect of Joule heating.

### Contact resistance

The actual contact area between two materials due to surface irregularities makes the equivalent resistance of the assembly to be strongly increased. Thus, contact resistances between the different pieces of the assembly have to be taken into account for accurate calculation. Because of the small spatial scale of surface irregularities (typically of micrometers (6)), contact resistances are modeled with an approach based on material interfaces. In other words, the contact resistance is defined on internal faces between two cells of the computational domain. Moreover, it is assumed that the contact resistance has a homogenous distribution on the interface between the two materials. For instance, if the total contact resistance between the bolt and the rib is  $1\mu\Omega$ ,

and the interface surface is  $10\text{mm}^2$ , the local contact resistance is  $10\mu\Omega/\text{mm}^2$ .

Contact resistance cause important voltage drop into the assembly. The following sketch (figure 3) illustrates the voltage drop dues to the contact resistance  $R_c$  between two materials. The two intrinsic resistances  $R_1$  and  $R_2$  are due to the materials electric conductivities. The electric current is constant along the circuit. Because the contact resistance  $R_c$  is distributed on a shorter length, it produces a stiff voltage drop  $R_c I$ . The electric power associated to the contact is assumed to be dissipated in materials through thermal fluxes exchanged on both sides of the contact. Once the temperature of the contact reaches a given value, the resistance of the contact decreases to a lower value. This phenomenon is not reversible.

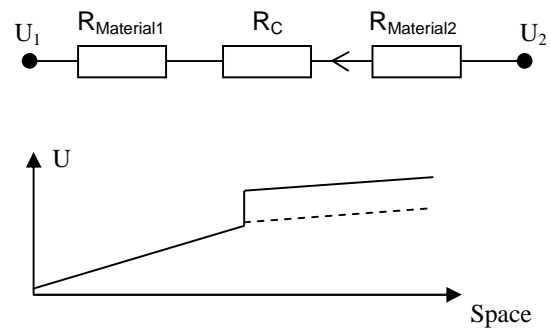


Fig. 3. Illustration of the voltage drop dues to contact resistance along a current path.

In the present model, the fusing temperature is defined by the lowest melting temperature of the materials on both side of the contact. For example, this temperature is about  $650^\circ\text{C}$  for aluminum. Concerning the contact between carbon composite and aluminum, it is assumed that the fusion of the contact is due to the melting of aluminum. The contact resistance after fusion is assumed to be one thousand times smaller than the initial value, which causes the voltage drop to vanish (dashed line on figure 3).

### ATTACHMENT

Attachment of lighting arc on fasteners during sweeping process is very likely. In this case, all the lightning current flows from the head of the screw to the structure across the fastening assembly. In this part, we present first the principle for the current injection in the structure. We also introduce the geometry and mesh used

for the calculation. Then, some important results are presented.

### Injection of current

Recent developments of a numerical model of the arc attachment during high current stage on unpainted metallic panels show that the arc root continuously expands in the radial direction (7). This expansion comes from the fluid flows associated with the explosion of the arc and the radiative transfers that heat the surrounding zones of the arc core. This expansion of the arc core on a panel is similar to the expansion of an infinite length arc column evolving freely in air (see figure 4). This evolution of the conductive radius over time is used for the current injection on the head of the screw. However, observation of front faces of painted assemblies after lightning tests indicates that the arc root size slightly exceed the radius of the screw head. Thus, in the present model, the arc root radius continuously expands until it reaches the radius of the screw head (typically half cm).

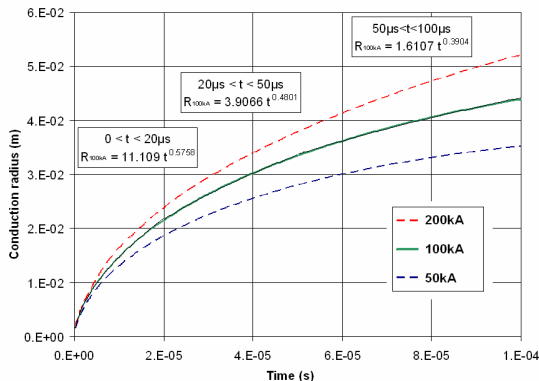


Fig. 4. Evolution of long lightning arc column radius over time for different currents (2D, D and D/2 waveforms)

After that time, the radius remains constant. The lighting current used for calculations is a D waveform (8). It reaches a radius of 5 mm few microseconds after arc ignition.

### Mesh and geometry

The computation domain is presented on figure 5. The current returns to the fictive generator through an additional metallic piece, represented in red. This feature is used to reduce the computation domain and the global inductance of the system. The rib doesn't connect to the current return piece all around the bolt in order to simulate

the effect of asymmetry in the rib. The mesh contains about 500000 cells, among them 150000 in the air zone. All the contact resistances are set to 5mΩ for this example.

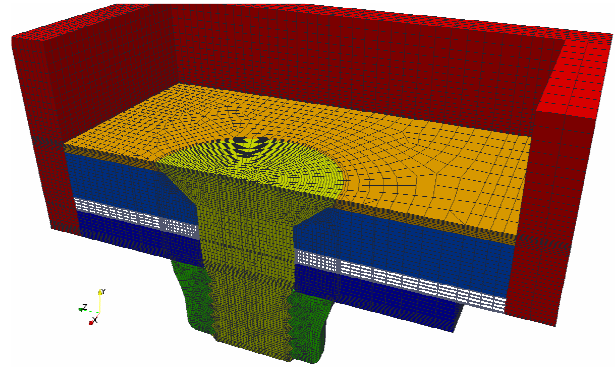


Fig 5. Computation domain (Orange: surface metallization; light blue: skin; white: insulator; blue: rib; yellow: screw; green: nut; red: return current piece)

### Effect of the rate of rise

In a first step, we present some electric characteristics of the assembly for a given rate of rise of the total current. On figure 6, we present the current distribution within the structure, on the left with a continuing current, on the right with a given current ramp ( $di/dt=1kA/\mu s$ ). Arc radius is assumed to be 1mm.

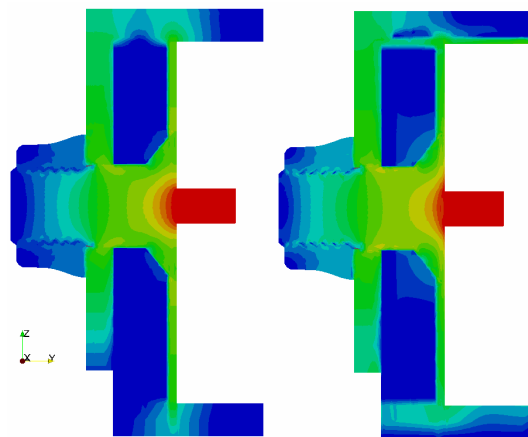


Fig. 6. Distribution of the dimensionless current within the assembly (log scale). Left: static approach. Right: quasi static approach

We can notice that static and transient approaches give similar results. The current flowing into the nut and the skin are about two times greater with transient approach. Skin effect is present into the return current piece, but it is negligible in regions close to the bolt. The voltage distribution into the assembly for quasi static approach shows also self induction effect: for the same total current, the voltage is about 3 times greater. This difference increases obviously with the value of the rate of rise of the total current. Calculations with higher rates of rise ( $>100\text{kA}/\mu\text{s}$ ) give intense electric field, especially in the zone around nut-rib contact. However, it is not sufficient to cause voltage sparking ( $<1\text{kV}/\text{mm}$ ). Anyway, if we consider the zone close to the fastener, calculations show that induction become negligible regarding voltage gradient when the rate of rise become lower than few  $\text{kA}/\mu\text{s}$ . For that reason, calculation with quasi static approach is used during the first  $\mu\text{s}$ , when the rate of rise is important. After that time, static approach is used. By this way, calculation cost is reduced by a factor of 4.

### Effect of temperature

The temperature rise in the assembly is caused by Joule heating and thermal fluxes due to contact resistances. Thus, this rise is faster where the contact resistances play an important role, as illustrated on Figure 7, left. The temperature within the assembly  $40\mu\text{s}$  after ignition reaches the boiling point on these interfaces while the temperature at the center of the screw doesn't exceed  $100^\circ\text{C}$ . Temperature rise is particularly strong where current density is reinforced and contact resistance is important, as bolt-rib contact, and bolt-metallization contact. The temperature on the surface of the screw is caused by the thermal flux associated to the presence of the arc.

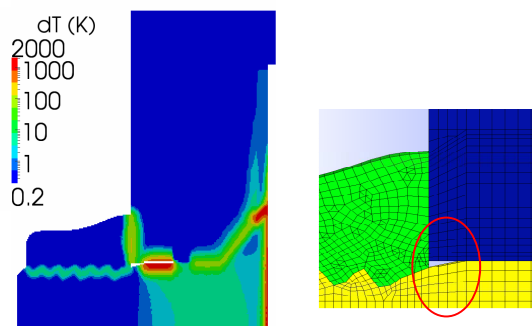


Fig. 7. Left: Distribution of the temperature into the assembly (log scale,  $t=40\mu\text{s}$ ). Right: internal void.

This field of temperature results from the choice of materials and the set of contact resistance. Moreover, this simulation has been performed with the presence of an internal void between screw and rib (see fig. 7, right, circled in red). This void causes the current density to be reinforced in the bolt-rib contact by a factor of 1.4, and the Joule heating by a factor 2. All of these features (high contact resistance, presence of voids, composite skin) lead to likely sparking occurrence.

Similar calculations with lower contact resistances, especially on bolt-rib interface doesn't give such temperature fields. Moreover, calculations with metallic skin (about one thousand times more conductive), indicates that the reinforcement of the current density on these two critical zones are highly mitigated.

### CONDUCTION

Conduction of lightning current in the fastener can causes sparking even if the current is lower that the total current. In this case, a part of the total current enters the bolt and exits in another piece of the structure (fuselage, rib, spar ...). In this part, we present the geometry and the mesh and then we present some important results.

### Mesh and geometry

The geometry considered for this example consists of two holed plates assembled with a screw and a nut (fig. 8). A voltage difference is applied across the assembly, causing a current to flow across it.

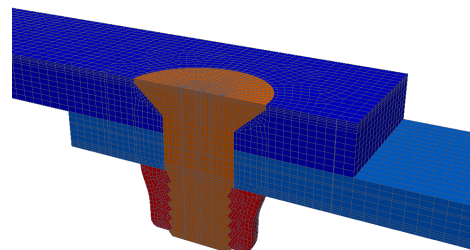


Fig. 8. Computation domain (Orange: screw; light blue: rib (al.); blue: skin (al.); red: nut)

The contact resistance between the upper plates (i.e. the skin) and the lower plate (i.e. the rib) is  $1\text{m}\Omega$ . All the others contact resistances have the same value. The two plates are aluminum, which means that their intrinsic resistances are low comparing to contact resistances. Thus, current distribution in the elements is essentially

determined by contact resistances. As result, we can predict that about the half part of the current should flow across the bolt  $I_b$ , and a half part of the current  $I_b$  should flow across the nut.

## Results

Results with quasi static approach show very complex current paths during the first microseconds. After that time, current streamlines converge to the path presented on upper picture of figure 9. After  $1\mu s$ , static calculation for electromagnetism is used. Most of current streamlines enters the screw, go down and flows into the lower plate, either directly, either after crossing the nut. We can notice that the amplitude of current density increases when it enters the screw because the conductive section decreases.

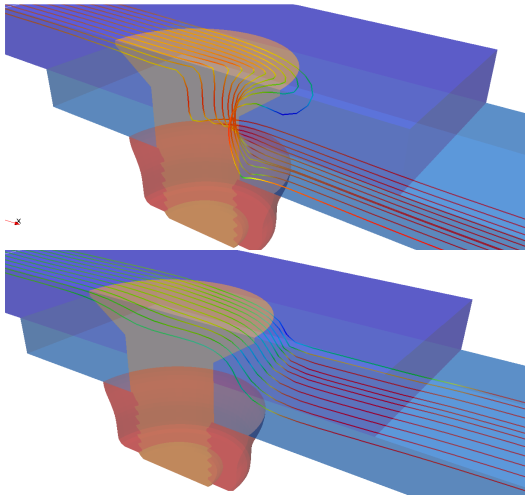


Fig. 9. Current streamlines in the assembly, colored by the amplitude, before and after the fusion of the contact.

The temperature increases and reaches the fusion point of the contact between the two plates. The evolution of the maximal temperature over time on the contact is presented on figure 10. We can notice that the rise is quite linear until the fusion of the contact. After that time, the thermal flux associated to the contact resistance is close to zero, and the thermal diffusion becomes greater than Joule heating. As a result, the temperature at the interface decays slowly after the fusion.

Moreover, after the fusion of the contact, most of the current streamlines flows directly from the upper plate to the lower plate. They avoid to flow across the screw (see fig. 11) because the

conductivity of titanium is 5 times smaller than aluminum (fig. 2). This feature mitigates the current density amplitude within the assembly.

The distribution of the current is also illustrated on figure 12, which shows the current flowing across each contact included in the model over time.

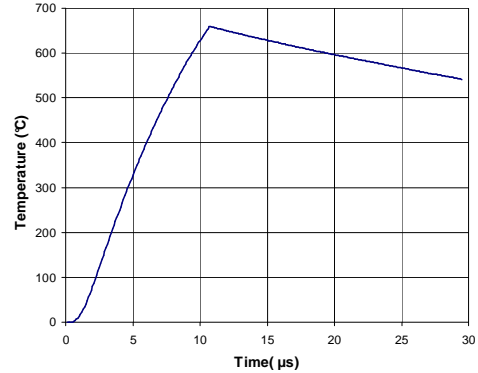


Fig. 10. Temperature of the skin-rib contact

Before the fusion of the contact (at  $t=10\mu s$ ), 60% of the current flows from the upper to the lower plate, as predicted with the analysis of the previous section (green curve). The current that enters to screw (blue curve) is divided in two equal parts, flowing either directly to the rib (purple curve) or across the nut (yellow). After the fusion of the contact, no current enters the bolt

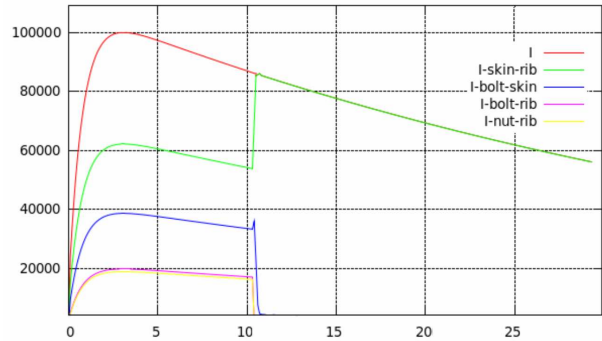


Fig. 11. Evolution of the current (A) over time (µs) in the assembly.

When the contact fuses, we can see that the current path instantaneously changes. This feature is due to the use of the static model, and the transition should be slower if transient model is used. Moreover, the fusing process is probably not instantaneous, and a new approach is under development. Compared to the previous case (attachment), no vaporization of the material occurs. Current densities are not so important, and the contact resistances heat the assembly in

a moderate way. Thus, in these conditions, no sparking should occur in this assembly.

## CONCLUSION

We have presented in this paper a thermo electric model dedicated to the simulation of sparking occurrence in fastening assemblies. The basic principle of the method consists in the incorporation of the all of the piece that constitutes the assembly into a 3D computation domain. This model is based on the heat equation to determine the temperature field within the structure, and a set of electromagnetic equations to calculate the current path. The contact resistances are also modeled with a surface approach and allow more realistic calculations of current distributions.

The model has been used to simulate the two cases in which the lightning current interacts with the assembly. The first situation is the direct attachment of the lightning arc on the head of the screw. Some distributions of current and temperature have been presented and discussed. The situation of current conduction across the assembly has also been presented.

One of the most important results brings to light with this tool is the important differences on the phenomenon for both configurations. While the current path remains approximately the same in attachment, the fusion of contacts in conduction causes an important modification of the current path and the heating within the structure. Moreover, calculations have shown that the rate of rise of the lightning current plays an important role in the current densities and voltage distribution.

## FUTURE PROSPECTS

The main goal of this tool is to help aircraft manufacturer in reducing the number of lightning tests to be perform for certification. There are more than one hundred different kinds of fasteners in fuel tank area. This large number comes from the different systems (rivet, screw, sleeves, countersunk or hexagonal head, floating or leak proof nut) and sizes (from 4 to 18 mm in diameters). This tool may be used for parametric analyses, for example on the effects of drill diameter, material thicknesses... Relative comparisons of results could be performed to determine the worst case that will be tested in laboratory ...

Moreover, the inherent defaults associated to these fasteners (e.g. mounting, ageing, in service incident...) have to be taken into account in the certification process, and they considerably increase the test matrix. In the future, this tool could be used to determine upper bound defaults that include several kinds of defaults (e.g. corrosion, presence of fragments, or absence of torque tightening...)

## REFERENCES

- (1) F. A. Fisher, J.A. Plumer and R.A. Perala, 'Lightning Protection of Aircraft' Lightning Technologies Inc., 1989.
- (2) I. Revel et al., 'Understanding of sparking phenomenon in CFRP assemblies', ICOLSE 2009.
- (3) L Chemartin et al., J. Phys. D: Appl. Phys. 44 (2011) 194003 (12pp)
- (4) Teulet et al., 'Calculation of the pressure build-up around a fastener due to sparking', ICOLSE 2011.
- (5) P Feraboli, M. Miller, 'Damage resistance and tolerance of carbon/epoxy composite coupons subjected to simulated lightning strike.' Composites: Part A 40 (2009) 954–967
- (6) S Schoft, 'Joint resistance depending on joint force of high current aluminum joints', Proceedings of the 22nd Conference on Electrical Contacts 2004, Seattle, pp. 502 - 510
- (7) L Chemartin et al., Direct Effects of Lightning on Aircraft Structure: Analysis of the Thermal, Electrical and Mechanical Constraints, Aerospace Lab. Journal, issue 05, 2012.
- (8) Aircraft Lightning Environment and Related Test Waveforms (ARP512, 1999).